International Journal of Concrete Structures and Materials

RESEARCH Open Access

Flexural Behavior Evaluation for Seismic, Durability and Structure Performance Improvement of Aged Bridge According to Reinforcement Methods

Tae-Kyun Kim[1*] and Jong-Sup Park[1]

Abstract

Among infrastructure, concrete bridges are the most exposed to various environmental effects. Structural degradation occurs due to natural and artificial influences shortening the lifespan of the structure. Therefore, bridges need to be reinforced over time. The structures used in this study are re-formed using aged bridge floor decks that have been used for 50 years, approximately. The fiber-reinforced polymer (FRP) adhesion method, using sheets and plate forms, was selected among various reinforcement methods to investigate the performance of reinforced structures. We have tested various reinforcement scenarios including one and two layers FRP sheets and FRP plates. The mechanical properties of the reinforced structures were evaluated experimentally through tensile strength and flexural test experiments. In contrast to most available literature focused on model-based studies, our present work represents an experimental test validation of structural reinforcement on an actual bridge. Our results indicate that fiber-based reinforcement in sheet form exhibits higher performances of the reinforced structure compared to reinforcement using the plate form. This study is intended to provide sufficient data for reinforcing bridge floors that could be used for reference at future construction sites.

Keywords Aged bridge deck, Reinforcement, CFRP sheet, CFRP plate, External adhesion method, Stiffness

1 Introduction

Concrete structures degrade over time (Shin, 2012; Shin et al., 2013). Degradation is caused by artificial factors such as fatigue, load, and vibration, alongside natural and environmental factors such as seasons, rain, and exposure to maritime environment at coastal locations (Mehta et al., 2006; Sidney et al., 2003). The degradation phenomenon induces weakness in concrete structures, cracks, and rebar corrosion, thus considerably reducing their durability, safety, and usability. Among infrastructure, bridge structures are particularly exposed to the environmental effects of various locations and environments, mainly because these structures are significantly affected by external degradation both directly and indirectly (Shin, 2012; Shin et al., 2013). Therefore, the degraded structures need to be reinforced over time. Various designs and methods are usually applied for reinforcing concrete bridges (Ministry, 2019). Examples of these methods include (1) the replacement method for restoring or enhancing load-carrying capacity by replacing or removing part or all of the degraded elements, (2) the cross-sectional expansion method for increasing the flexural moment accompanied by the increase of the neutral axis attributed to the compression of the concrete

Journal information: ISSN 1976-0485 / eISSN 2234-1315.

*Correspondence:
Tae-Kyun Kim
kimtaekyun@kict.re.kr
Full list of author information is available at the end of the article

bridge's upper plate and improvement of the load resistance to the shear, and (3) the concrete winding method that increases the load-carrying capacity of the degraded element by adding concrete around the existing concrete or wrapping it with stiffener. However, in the case of flexural and shear reinforcement, the review of the application process by a professional technician is necessary (Ministry, 2019). Additional reinforcement methods include the longitudinal girder extension method that reduces the moment and shear force by adding girder to slabs such as bridge floor decks, the support method that reduces the working force by establishing new piers and support points inside the span and shortening the span, the steel sheet reinforcement method in which steel sheets are installed on concrete members and integrated with existing members to improve performance, the fiber reinforcement method that improves member performance by bonding fibers and plate shapes to concrete member surfaces, and the external prestressing method that introduces prestress for flexural and shear reinforcement of concrete bridges (Fan et al., 2019; Herbrand & Classen, 2015; Ministry, 2019; Pisani, 2018; Yang et al., 2018). Among these various reinforcement methods, the steel sheet and the fiber reinforcement methods are the most widely studied and applied (Firmo & Correia, 2015; Franco et al., 2018; Mathew & Prabhakaran, 2018; Mostofinejad & Moshiri, 2015; Tajmir-Riahi et al., 2019). In the case of the steel sheet reinforcement method, the material properties of the steel sheet are well presented. However, challenging construction difficulties related to problems such as weight hinders the ease of application for this method for large structures (Kim et al., 2008). Therefore, the fiber reinforcement method is mainly used when the area is large and is consequently the most widely commercialized method (Bilotta et al., 2015; Kim et al., 2008; Moshiri et al., 2020; Triantafyllou et al., 2018). In this study, the fiber reinforcement method is applied to actual structures degraded due to aging (Correia et al., 2017; Khalifa, 2016). The materials commonly used in the fiber reinforcement method are mainly glass fiber reinforced polymer (GFRP), Aramid fiber reinforced polymer (AFRP), and carbon fiber reinforced polymer (CFRP) (Kim et al., 2010; Kishi et al., 2020). These various materials have different physical properties. Among them, CFRP exhibits relatively higher tensile strength and elastic modulus compared to GFRP and AFRP (Ali et al., 2021; Bakalarz & Kossakowski, 2019; Brózda et al., 2017; Kim et al., 2010). Therefore, the CFRP with the best performance is used for reinforcement in the form of plates with several sheet layers. As such, the most important parameter for reinforcement is the adhesion between CFRP and concrete interfaces, which plays a key role in its integrated behavior. The mechanical performance of CFRP reinforcement in a plate form is initially identified using measurements of tensile properties, before its attachment to concrete structures. Several studies on CFRP reinforcement have been reported in the literature. Zhang et al. (2015) experimentally compared and analyzed the performance of a 1200 mm arched concrete model beam by setting variables according to thickness in the form of CFRP sheet and strip. Helal et al. (2020) evaluated the flexural performance of 150×300 mm RC specimens according to the content rate of steel fiber and synthetic fiber and the attachment of the CFRP sheet. Salama et al. (2019) evaluated the structural flexural performance according to the number of files and the reinforcement of the CFRP sheet on the bottom and side surfaces of a 2 mm beam tension side of the RC. Jawdhari et al. (2018) evaluated and compared the structural performance of a 3 m RC beam of 150×150 mm according to the thickness of the tensile side CRP and the overlapping variables of the tensile side reinforcement specimens and CFRP tensile side. Al-Khafaji et al. (2020) compared and analyzed the performance of a T-beam before and after performing a three-panel-point experiment by adding CFRP reinforcement and introducing the width and number of layers as variables to their model structure in reverse using the 3 m RC structure of the T-beam (Al-Khafaji et al., 2020; Helal et al., 2020; Jawdhari et al., 2018; Salama et al., 2019; Zhang et al., 2015). Reported works on CFRP reinforcement methods have been mainly conducted on calculated models considering non-degradable and small structures. The main element of differentiation in our present paper is the fact that we have evaluated the performance by applying the CFRP method to real degraded structures that have been used for decades. Therefore, in this study, CFRP are used, considering various environmental, chemical, and strength aspects observed in previous research. CFRP possess several advantages that conventional metallic materials do not have, such as high specific strength, tensile strength, modulus of elasticity, low thermal expansion coefficient, and high fatigue strength.

To this end, this study analyzes the flexural performance of a floor deck structure reinforced with one and two layers FRP sheet, and two layers of FRP plate on the bottom surface using the floor deck that receives the most vehicle load among the various parts of the aged bridge. The performances of all the above cases are compared to the performance of the floor deck structure with no reinforcement. A material physical property test of the FRP reinforcing material was also performed to improve the accuracy in these experiments. Although most of the previous studies were focused on reinforcing small-scale or un-degraded structures, this study aims at reinforcing aged bridges

by performing proper stiffness and behavior analyses and comparing results to those of unreinforced bridge specimens. Thus, this study is intended to provide a sufficient set of data for reinforcing floors that could be used for reference at future construction sites.

2 Materials and Methods

The target bridge used in this study is a bridge located in Gangneung-si, Gangwon-do, South Korea. The bridge was completed in September 1975 as a two-lane bridge and has been used for just under 50 years. The superstructure form is PSC-I, with a short-span and span composition of approximate widths of 26.3 m and 11.8 m, respectively. In addition, the effective width, height, and maximum diameter of the bridge are 7.2 m, 7 m, and 25 m, respectively. Finally, the total number of spans of the bridge is one, and the design load is DB-24.

2.1 Test Specimens Remolding

A 3000×1650×210 mm piece has been extracted from the bottom deck of the aged bridge as a test specimen. Before taking measurements, the test specimen is reformed, as shown in Fig. 1, to make four specimens cut into 125×1650×210 mm sizes as shown in Fig. 2. Only one tension bar was arranged at the center of the bottom end to maintain the same experimental conditions during structural measurements.

The reason for longitudinally shaping the specimen as shown in Fig. 2 is related to the direction of vehicle movement and the support points of the floor deck. This study aims to assess the maximum flexural performance of the floor panel due to vehicle passage. Therefore, the specimen was reshaped as shown in Fig. 2 to confirm the condition where both ends of the existing floor panel act as support points.

2.2 Concrete Strength Test Method

Before the structural test, the concrete strength test is performed first, as shown in Fig. 3. In this case, a concrete core test sample is collected from the floor deck and

Fig. 1 Concrete deck remolding

Fig. 3 Concrete compressive strength test

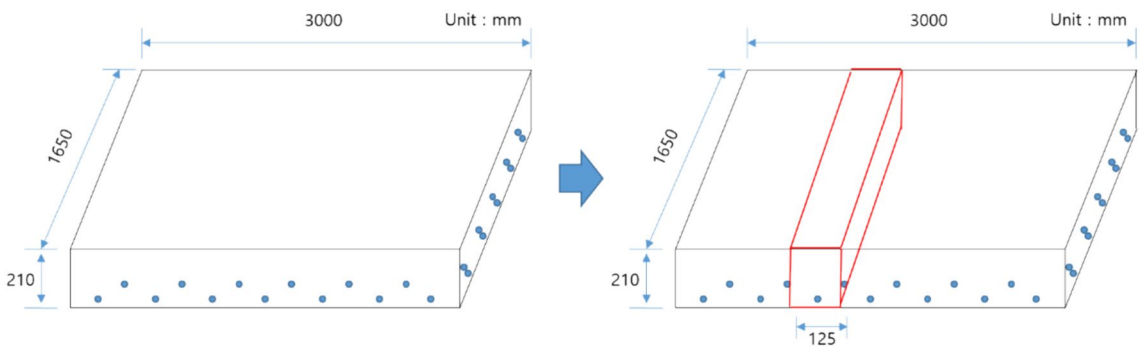

Fig. 2 Concrete deck remolding detail

Table 1 FRP sheet tensile specimens' details

Section	Description	Size (mm)
L3	Total length	250
L2	Distance between reinforcing bands	150 ± 1
b1	Width-to-width distance	25 ± 0.5
h	Thickness	2 ± 0.2
L0	Point-to-point distance	50 ± 1
L	Bite-to-bite distance	136
LT	Length of reinforcing band	> 50
HT	Thickness of reinforcing band	0.5 ~ 2

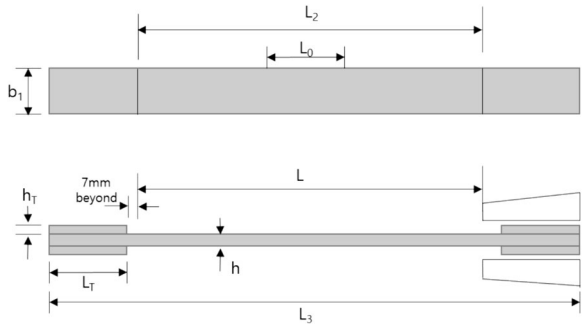

Fig. 4 Dimensional parameters of the FRP sheet tensile specimens (KS M ISO527, 2012)

compressive strength and splitting tensile strength tests are performed, according to KS F 2405 (Standard test method for compressive strength of concrete) and KS F 2423 (Standard test method for splitting tensile strength of concrete), respectively (KS F 2405; KS F 2423). Compressive strength and splitting tensile strength tests apply loads to 100 × 200 mm test specimens, vertically and horizontally depending on the test method. 1000 kN UTM (Universal Testing Machine) is used as test equipment.

2.3 CFRP Tensile Strength Method

A tensile strength experimental test is conducted on the CFRP sheet used in this study, according to the KS M ISO 527–5 (Plastics-Determination of tensile properties-Part 5: Test conditions for unidirectional fiber-reinforced plastic composite) standard. Two types of FRP sheets (one layer and two layers) are used for this experiment. Twenty specimens are tested for each FRP sheets type. The overall length of the specimen is 250 mm with a thickness of 2 ± 0.2 mm and a width approximately equal to 25 ± 0.5 mm, as shown in Table 1. Both sides of the individual test specimen should be parallel within 0.2 mm, as shown in Fig. 4, and both ends should be reinforced with reinforcing bands. In this case, the reinforcing band should be made of a cross-laminated plate or a glass fiber/resin laminated plate, such that the fiber direction is ± 45° with respect to the axis of the test specimen. Importantly, the ends should maintain a thickness in the range of 0.5 to 2 mm, and an angle at the edge equal to 90°. However, different reinforcing treatment methods are allowed, with the condition of maintaining the same length as before and keeping the variation coefficient in the same order of magnitude as for the recommended reinforcing band. Other methods include reinforcing bands made of the same material as the specimen, reinforcing bands in which mechanical tightening is enabled, and non-bonding reinforcing bands made of rough surface materials (using abrasive paper, sandpaper, and rough surface bite). To manufacture a specimen, an FRP sheet was cut and prepared by mixing with EPONDEX resin to perform impregnation in one layer and two layers. After more than 7 day of natural curing to secure strength, it was cut to 250 mm in length and 25 mm in width according to KS M ISO 527–5 standard (KS M ISO527, 2012). Furthermore, the FRP-based reinforcing band was cut into 50 mm in length and 25 mm in width, and the surface of the specimen and reinforcing band was roughened with sandpaper. Finally, the two layers of the reinforcing bands were bonded with an instantaneous adhesive, and the reinforcing band was reattached to the specimen.

A tensile test was performed using a 100 kN-capacity UTM and the response of the specimen was measured through a strain sensor attached to its center. After the distance between bites was marked as 136 mm, the reinforcing band part was fixed to ensure non- eccentricity using UTM with a capacity of 100 kN. Subsequently, the experiment was carried out until fracture with a displacement control of 1 mm/min according to KS M ISO 527–5 standard (KS M ISO527, 2012).

2.4 CFRP Strengthening Method

Fig. 5 shows a specimen according to the reinforcement method. The specimen size was kept the same. An unreinforced control specimen is shown in Fig. 5(a) for reference. Various reinforcement configurations corresponding to one and two layers of CFRP sheet are illustrated in Fig. 5(b, c), respectively. Fig. 5(d) shows the reinforcement with a CFRP plate. The layered CFRP sheet adhered to the specimen using liquid epoxy, while the CFRP plate adhered using a putty type epoxy. A 1-month curing period was sufficient. The reinforcement length was 1440 mm, corresponding to 90% of the length of the support point at both ends, i.e., 1600 mm.

2.5 Flexural Experimental Method

Fig. 6 presents the installed sensors' locations on the specimen and illustrates the experimental method

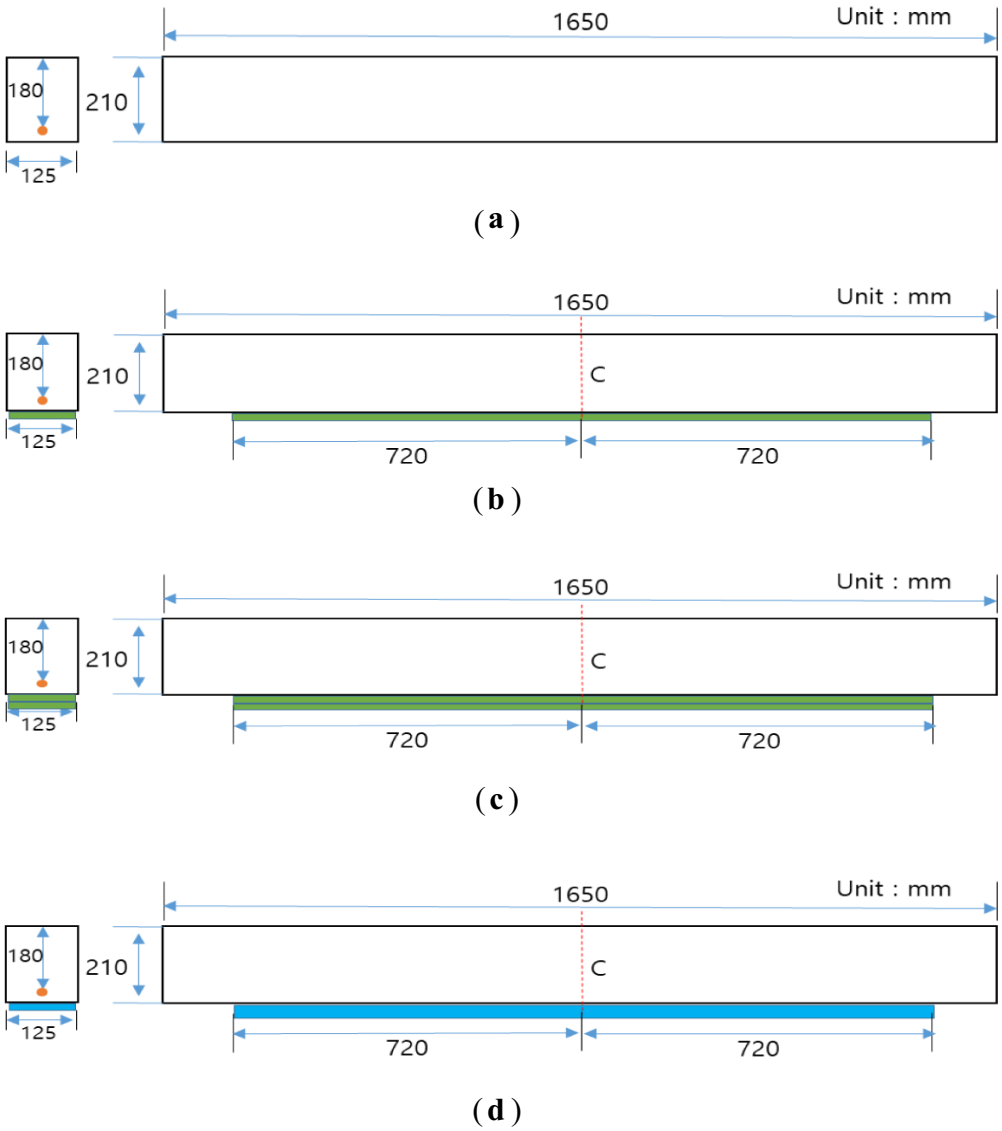

Fig. 5 Strengthening methods: **a** control; **b** CFRP sheet 1 layer; **c** CFRP sheet 2 layers; **d** CFRP plate

for the structural experiment. A UTM with a maximum load capacity of 5000 kN and a maximum stroke of 750 mm was used as loading equipment for applying loads to the test specimen. In the experimental method, the point distance was set at 1600 mm with a three-point load. The load was applied using a hydraulic press at the center position. The experiment was carried out with displacement control of 1 mm/min until the specimen was destroyed. To measure the vertical displacement when applying a load to a test specimen, one DT displacement meter was installed at each of the L/4, L/2, and 3L/4 points. To measure the strain, the height of 210 mm was divided into four equal parts at the center of the side surface, and S1 to S5 were sequentially installed from the top at equal intervals. Moreover, rebar strain sensors (B1 to B3) were installed at each of the L/4, L/2, and 3L/4 points based on the point distance at the bottom part.

2.6 Test Results

2.6.1 Concrete Strength Test Results

Table 2 shows the compressive strength and splitting tensile strength of the aged bridge floor deck. A total of three test specimens were used. However, in the compressive strength test, only two test specimens were measured due to errors. It was identified that the compressive strength of concrete was 36 and 40 MPa, with an average of 38 MPa. The splitting tensile strength was found

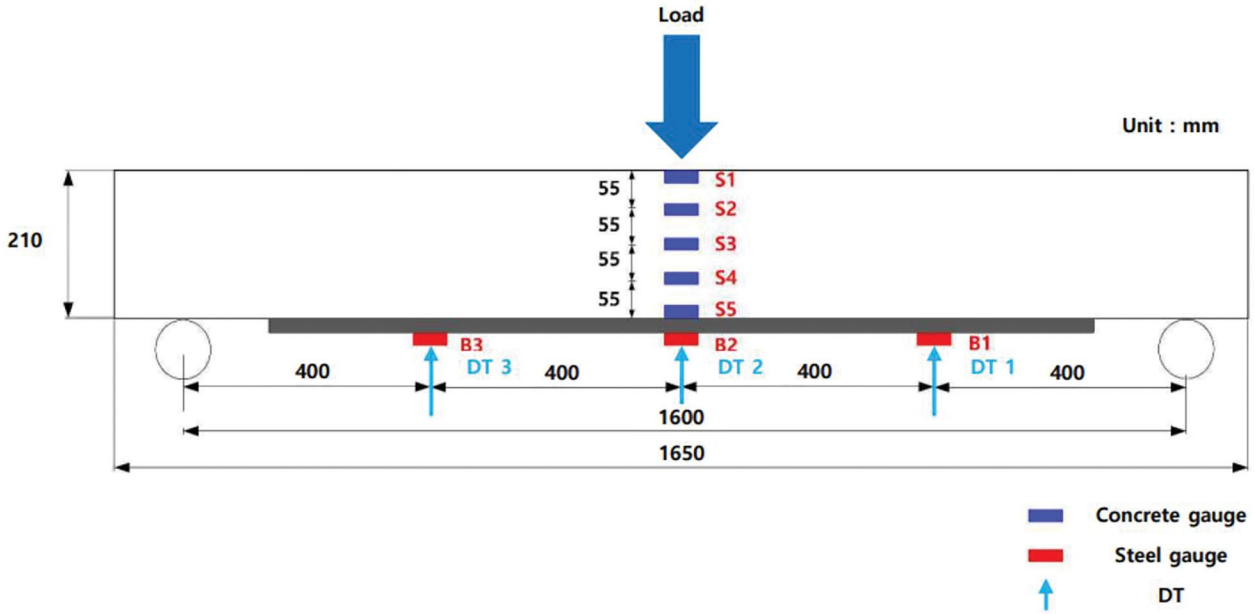

Fig. 6 Flexural test method

Table 2 Compressive strength and splitting tensile strength of the deck

No	Deck			
	Compressive		Splitting Tensile	
	Load(kN)	Strength(MPa)	Load(kN)	Strength(MPa)
1	285	36	82	4
2	317	40	108	5
3	–	–	107	5
Avg	301	38	99	4.6

to be 4, 5, and 5 MPa, with an average of 4.6 MPa. It was confirmed that the splitting tensile strength was normally 1/9–1/13 of the compressive strength.

2.6.2 CFRP Tensile Strength

Table 3 shows the tensile strength test results of one layer and two layers of the CFRP sheet. In the case of a single layer sheet, the maximum load and elastic modulus were found equal to 11.38 kN and 51.37 GPa, respectively. The maximum load and elastic modulus of the double layer sheet were found to be 12.98 kN and 111.75 GPa, respectively. The maximum load and elastic modulus of the two-layer sheet are approximately 1.14 and 2.18 times higher than the one-layer sheet, respectively. Based on the result of measuring the thickness using the Vernier Calipers, the average thickness of one layer was 0.81 mm and the average thickness of two layers was 1.51 mm. It was observed that the one-layer sheet showed a central fracture during the tensile test, while the two-layer sheet had an inter-layer slipping phenomenon in most cases. Thus, if CFRP and two-layer sheet show proper adhesion performance, they will show more improved tensile performance.

2.6.3 Flexural Experimental Test Results

Table 4 presents the displacement of each specimen as a function of the applied load. Load–displacement curves are shown in Fig. 7. Table 5 shows the load increase rate at the maximum load for each reinforcement test specimen compared to non-reinforcement. The maximum loads of non-reinforcement, CFRP sheet (1), CFRP sheet (2), and CFRP plate are 27.75, 48.00, 59.75, and 29.90 kN, respectively. The maximum load of each reinforcement test specimen increased by 1.78, 2.21, and 1.11 times, respectively, compared to the unreinforced test specimen. Moreover, the maximum displacement at the maximum load was found to be 3.71, 4.48, 6.10, and 2.68 mm, respectively. The stiffnesses up to an initial displacement of 2 mm, which is yield load, of the CFRP plate, CFRP sheet (1), and CFRP sheet (2) increase approximately by 1.25, 1.90, and 2.70 times, respectively, compared with the unreinforced test specimen. Furthermore, the ductility was secured in the order of sheet (2), sheet (1), and plate up to the maximum load after the yield point. In the case of the destruction mode, the sheet appears in the form of adhesion destruction, and the plate appears

Table 3 Tensile strength results of CFRP Sheet 1 and 2 layers

Sheet (1 l year)	Max load (kN)	Young's modulus (GPa)	Thickness (mm)	Sheet (2 l year)	Max Load (kN)	Young's modulus (GPa)	Thickness (mm)
1	9.19	45.75	0.72	1	16.73	120.41	1.51
2	15.30	51.77	0.77	2	10.43	126.81	1.46
3	17.22	42.39	0.82	3	19.21	103.63	1.38
4	6.43	52.75	0.83	4	15.16	126.24	1.45
5	16.19	49.34	0.77	5	12.69	99.82	1.49
6	9.37	49.91	0.80	6	3.86	115.13	1.58
7	13.72	48.49	0.76	7	9.61	111.78	1.51
8	15.11	51.87	0.86	8	5.89	111.89	1.37
9	7.65	42.45	0.83	9	12.59	107.17	1.48
10	10.10	47.07	0.82	10	17.22	92.17	1.40
11	5.33	46.43	0.84	11	12.93	103.47	1.46
12	8.85	53.77	0.81	12	10.99	94.54	1.45
13	11.09	34.12	0.87	13	9.92	95.84	1.54
14	13.91	65.02	0.78	14	15.73	112.11	1.75
15	14.09	52.49	0.79	15	20.60	166.65	1.59
16	11.05	62.48	0.86	16	17.41	109.77	1.72
17	8.22	53.08	0.80	17	12.98	101.13	1.62
18	13.11	70.37	0.77	18	11.27	106.44	1.47
19	9.48	56.07	0.87	19	9.91	99.97	1.45
20	12.18	51.76	0.86	20	14.39	129.94	1.54
Avg	11.38	51.37	0.81	Avg	12.98	111.75	1.51

Table 4 Test results details of specimens

Specimens	Load (kN)	DT1 (mm)	DT2 (mm)	DT3 (mm)
Control (Non-strengthening)	27.75	3.30	3.71	3.27
CFRP sheet (1)	48.00	2.79	4.48	4.71
CFRP sheet (2)	59.75	2.95	6.10	1.95
CFRP plate	29.90	1.77	2.68	2.37

Table 5 Maximum load comparison of specimens

Specimens	Load (kN)	Load increase rate compared with non-reinforcement (%)
Control (Non-strengthening)	27.75	–
CFRP sheet (1)	48.00	72.97
CFRP sheet (2)	59.75	115.32
CFRP plate	29.90	7.75

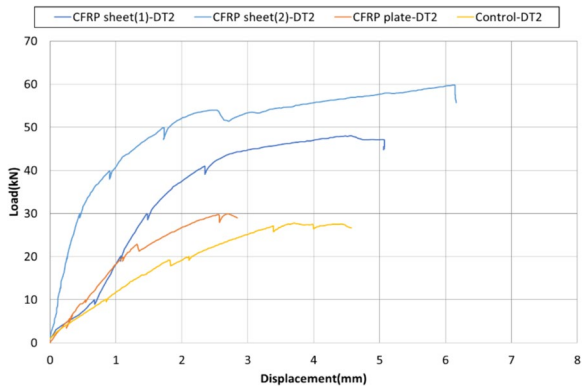

Fig. 7 Load–displacement of the flexural test

in the form of shear destruction. We observe that the reinforcement effect certainly appears when comparing the degraded floor deck with the unreinforced test specimen and test specimens processed with various reinforcement methods. In particular, the present results clearly show that the performance in the case of CFRP sheet reinforcement is remarkable. However, in the case of plate reinforcement, performance was not significantly improved. For this reason, the plate-reinforcement test specimen in this case did not undergo adhesion destruction. Instead, shear destruction proceeded near the point, and cracks were generated in the longitudinal direction at a height of about the middle of the beam leading to the end of the experiment. In

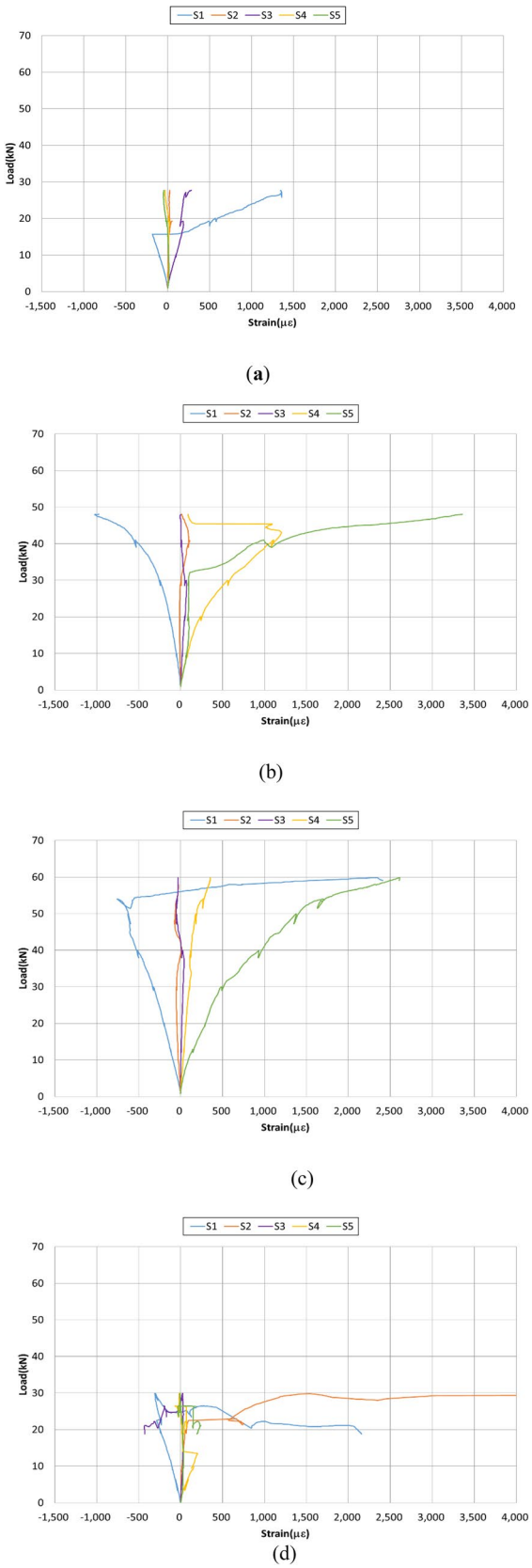

◀ **Fig. 8** Load—Strain of specimen: **a** control; **b** CFRP sheet 1 layer; **c** CFRP sheet 2 layers; **d** CFRP plate

the aged bridge floor deck used in this study, the concrete floor was reinforced once more during the period of use, and hence, it is judged that this phenomenon occurred due to a problem in the interface between the existing concrete floor and the new concrete floor. Plate reinforcement is judged to have a significant reinforcement effect similar to sheet reinforcement when the floor deck performs integrated behavior.

Fig. 8 presents the concrete load–strain curve for each test specimen variable. The compressive fracture strain of concrete is 0.003. Fig. 8(a) shows the results of an unreinforced specimen. The uppermost S1 concrete strain gauge changes drastically at a point with a load of about 15 kN. Additionally, the tensile strain gauge rapidly changes at the load of 45 kN in Fig. 8(b), and the compressive strain gauge shows a steady occurrence of the strain. Fig. 8(c) shows an abrupt and strong variation on the strain gauge at the early start of the test in both compression and tension. In Fig. 8(d), both compression and tension are observed to change rapidly at 25 kN points. Overall, the upper part represents a compression strain form and the lower part represents a tensile strain form. In particular, the unreinforced test specimen and the CFRP plate reinforced test specimen exhibit a compression destruction form. Compression destruction is a dangerous form as it represents the brittle behavior of the structure. And the reason for this is that the floor deck used in this study is a concrete reinforced floor deck, and the concrete on the top of the floor deck is expected to have lower strength than the lower concrete.

Table 6 presents the calculation results of the amount of movement of the neutral axis obtained using a lateral strain sensor. The neutral axis position was determined by calculating the girder height at which the strain curve for each height passes through the strain 0 points according to the load for each attachment position of the subject strain sensor. The unreinforced test specimen shows a pattern in which the height of the neutral axis rises sharply at the loading position and then decreases again as the load increases. CFRP sheet (1) shows a tendency that the height of the neutral axis gradually decreases at the loading position and then increases again as the load increases. CFRP sheet (2) shows a pattern in which the height of the neutral axis gradually decreases at the loading position and then increases again as the load increases. Finally, the CFRP plate shows a pattern in which the neutral axis position rapidly rises at the loading position and then decreases again as the load increases.

Table 6 Neutral axis position according to load using strain

Load (kN)	Specimens height (mm)—Reference point at the bottom of the specimen			
	Control (Non-strengthening)	CFRP sheet (1)	CFRP sheet (2)	CFRP plate
10	52.92	70.71	106.45	55.01
20	187.65	65.15	96.02	43.04
27	158.24	–	–	–
30	–	54.56	89.38	11.04
40	–	46.31	54.05	–
48	–	54.20	–	–
50	–	–	121.96	–
60	–	–	114.42	–

3 Conclusions

In this study, a fiber reinforcement method was applied to an aged bridge floor deck. FRP sheet (one, two layers) and plate were used for reinforcement. A tensile force test was performed to investigate the performance of the reinforced structure's specimens. Based on the results of the flexural experiment after reinforcement, we draw the following conclusions.

(1) Based on the results of performing a one- or two-layer tensile test on the CFRP sheet, it was confirmed that the maximum load of the two-layer specimen increased 1.14 times and the elastic modulus approximately doubled. However, as most of the two layers showed inter-layer slipping phenomena, higher tensile strength could be expected if attached properly.
(2) As a result of the flexural tests after reinforcement using the FRP sheets (1), (2), and FRP plate, the stiffness increased(Initial displacement: 2 mm) by approximately 1.25, 1.9 and 2.7 times compared to the unreinforced test specimen. In particular, the FRP sheet reinforcement showed a reliable reinforcement effect, while the plate showed an insufficient reinforcement effect.
(3) The maximum load increases the load by 1.78, 2.21, and 1.11 times, respectively, compared to the control test specimen. The reinforcement effect of the FRP sheet is certain. In the tensile material experiment, a number of slips occurred in CFRP sheet (2), but the reinforcement effect is the greatest.
(4) The maximum sagging at the bottom plate center increases by 1.20, 1.64, and 0.44 times compared to the control test specimen, respectively. In this way, the sheet moved more integrally than the plate, and two layers were more stably judged than one layer.
(5) The flexural experiment results showed that adhesion destruction and FRP dropout shapes appeared in all test specimens. Therefore, higher performance can be expected when integrated with the concrete floor deck structure after proper reinforcement. Further research is needed to improve adhesion performance using anchors or various types of epoxy materials.
(6) In this study, an aged bridge floor deck that receives the most vehicle load was used. Moreover, the reinforcement method was limited to one type of adhesion method and carbon fiber. Therefore, in future studies, more accurate comparison and analysis results can be deduced by performing research utilizing various components of aged bridges, using various reinforcement methods such as external tensioning method and cross-section expansion method, using various fibers such as GFRP and AFRP, and using various stiffeners such as rebar and steel strand. Furthermore, the results of this study are available as data when reinforcing degraded bridges.

Acknowledgements
Research for this paper was carried out under the KICT Research Program (project no. 20240083-001, Development of Eco-Friendly Carbon Eating Concrete (CEC) Manufacturing and Utilization Technology) funded by the Ministry of Science and ICT.

Author contributions
Tae-Kyun Kim: conceptualization, methodology, validation, formal analysis investigation, resources, data curation, writing—original draft, writing—review and editing, visualization. Jong-Sup Park: supervision, project administration, funding acquisition.

Funding
Research for this paper was carried out under the KICT Research Program (project no. 20240083–001, Development of Eco-Friendly Carbon Eating Concrete(CEC) Manufacturing and Utilization Technology) funded by the Ministry of Science and ICT.

Availability of data and materials
Data will be made available on reasonable request.

Declarations

Ethics approval and consent to participate
All authors of the manuscript confirm ethical approval and consent to participate following the Journal's policies.

Consent for publication
All the authors agree that the article will be published after acceptance.

Competing interests
The authors declare that they have no known competing financial interests or personal relationships that could have appeared to influence the work reported in this paper.

Author details
[1]Department of Structural Engineering Research, Korea Institute of Civil Engineering and Building Technology, Daehwa-Dong, Goyang-Si, Gyeonggi-Do 10223, Republic of Korea.

Received: 4 February 2024 Accepted: 28 April 2024
Published online: 09 August 2024

References

Ali, H., Assih, J., & Li, A. (2021). Flexural capacity of continuous reinforced concrete beams strengthened or repaired by CFRP/GFRP sheets. *International Journal of Adhesion and Adhesives, 104*, 102759.
Al-Khafaji, A., & Salim, H. (2020). Flexural strengthening of RC continuous T-beams using CFRP. *Fibers, 8*, 41.
Bakalarz, M., & Kossakowski, P. (2019). The flexural capacity of laminated veneer lumber beams strengthened with AFRP and GFRP sheets. *Technical Transactions, 116*, 85–95.
Bilotta, A., Ceroni, F., Nigro, E., & Pecce, M. (2015). Efficiency of CFRP NSM strips and EBR plates for flexural strengthening of RC beams and loading pattern influence. *Composite Structures, 124*, 163–175.
Brózda, K., Selejdak, J., & Koteš, P. (2017). The analysis of beam reinforced with FRP bars in bending. *Procedia Engineering, 192*, 64–68.
Correia, L., Sena-Cruz, J., Michels, J., França, P., Pereira, E., & Escusa, G. (2017). Durability of RC slabs strengthened with prestressed CFRP laminate strips under different environmental and loading conditions. *Composites Part B: Engineering, 125*, 71–88.
Franco, N., Biscaia, H., & Chastre, C. (2018). Experimental and numerical analyses of flexurally-strengthened concrete T-beams with stainless steel. *Engineering Structures, 172*, 981–996.
Fan, Y., Chen, L., Fang, Q., & Wang, T. (2019). Blast resistance of externally prestressed RC Beam: A theoretical approach. *Engineering Structures, 179*, 211–224.
Firmo, J. P., & Correia, J. R. (2015). Fire behaviour of thermally insulated RC beams strengthened with EBR-CFRP strips: Experimental study. *Composite Structures, 122*, 144–154.
Helal, K., Yehia, S., Hawileh, R., & Abdalla, J. (2020). Performance of preloaded CFRP-strengthened fiber reinforced concrete beams. *Composite Structures, 244*, 112262.
Herbrand, M., & Classen, M. (2015). Shear tests on continuous prestressed concrete beams with external prestressing. *Structural Concrete, 16*, 428–437.
Jawdhari, A., Peiris, A., & Harik, I. (2018). Experimental study on RC beams strengthened with CFRP rod panels. *Engineering Structures, 173*, 693–705.
Khalifa, A. M. (2016). Flexural performance of RC beams strengthened with near surface mounted CFRP strips. *Alexandria Engineering Journal, 55*(2), 1497–1505.
Kim, S. B., Kim, J. H. T., Nam, J. W., Kang, S. H., & Byun, K. J. (2008). Bond-slip model of interface between CFRP sheets and concrete beams strengthened with CFRP. *Journal of the Korea Concrete Institute, 20*, 477–486.
Kim, Y. J., Yoo, D. Y., Lee, S. K., Kim, M. H., & Yoon, Y. S. (2010). *Analytical Study on Concrete Strengthened with FRP Sheet under Low-velocity Impact Loading. In Proceedings of the Korea Concrete Institute Conference*, 159–160
Kishi, N., Komuro, M., Kawarai, T., & Mikami, H. (2020). Low-velocity impact load testing of RC beams strengthened in flexure with bonded FRP sheets. *Journal of Composites for Construction, 24*, 04020036.
KS F 2405. (2010). *Standard test method for compressive strength of concrete, Korea Standards Association* (KSA), Seoul, KR.
KS F 2423. (2016). *Standard test method for splitting tensile strength of concrete, Korea Standards Association* (KSA), Seoul, KR.
KS M ISO 527. (2012). *Plastics-Determination of tensile properties-Part 5 : Test conditions for unidirectional fiber-reinforced plastic composite, Korea Standards Association* (KSA), Seoul, KR.
Mathew, M. J., & Prabhakaran, P. (2018). Combined EBR and NSMR for flexural strengthening of RC beams. *International Research Journal of Engineering and Technology (IRJET), 5*, 2395–2472.
Mehta, P. K., & Paulo, J. M. M. (2006). *Concrete Microstructure, Properties, and Materials* (3rd ed.). McGraw Hill.
(2019). *Ministry of Land, infrastructure, and transport. Study on the preparation of maintenance and reinforcement guidelines for facilities (Bridges, Tunnels, etc.)*. (Report No. RD-19-R3–001, Korea Authority of Land & Infrastructure Safety, Jinju, Gyeongnam.
Mostofinejad, D., & Moshiri, N. (2015). Compressive strength of CFRP composites used for strengthening of RC columns: comparative evaluation of EBR and grooving methods. *Journal of Composites for Construction, 19*, 04014079.
Moshiri, N., Czaderski, C., Mostofinejad, D., Hosseini, A., Sanginabadi, K., Breveglieri, M., & Motavalli, M. (2020). Flexural strengthening of RC slabs with nonprestressed and prestressed CFRP strips using EBROG method. *Composites Part B: Engineering, 201*, 108359.
Pisani, M. A. (2018). Behaviour under long-term loading of externally prestressed concrete beams. *Engineering Structures, 160*, 24–33.
Salama, A. S. D., Hawileh, R. A., & Abdalla, J. A. (2019). Performance of externally strengthened RC beams with side-bonded CFRP sheets. *Composite Structures, 212*, 281–290.
Shin, H. M. (2012). *Prestressed Concrete* (10th ed.). Dong Myeong. Paju City.
Shin, H. M., & Lee, J. H. (2013). *Reinforced Concrete* (11th ed.). Dong Myeong. Paju City.
Sidney, M., Francis, Y., & David, D. (2003). *Concrete* (2nd ed.). Prentice Hall.
Tajmir-Riahi, A., Moshiri, N., Czaderski, C., & Mostofinejad, D. (2019). Effect of the EBROG method on strip-to-concrete bond behavior. *Construction and Building Materials, 220*, 701–711.
Triantafyllou, G. G., Rousakis, T. C., & Karabinis, A. I. (2018). Effect of patch repair and strengthening with EBR and NSM CFRP laminates for RC beams with low, medium and heavy corrosion. *Composites Part B: Engineering, 133*, 101–111.
Yang, D. H., Kwon, M. J., Eom, G. H., & Kim, J. H. J. (2018). RC arch deck development and performance evaluation for enhanced deck width. *International Journal of Concrete Structures and Materials, 12*, 1–20.
Zhang, X., Wang, P., Jiang, M., Fan, H., Zhou, J., Li, W., Dong, L., Chen, H., & Jin, F. (2015). CFRP strengthening reinforced concrete arches: Strengthening methods and experimental studies. *Composite Structures, 131*, 852–867.

Publisher's Note

Tae-Kyun Kim Ph.D., Researcher, Structural Engineering Research, Korea Institute of Civil Engineering and Building Technology, Republic of Korea.

Jong-Sup Park Ph.D., Research Fellow, Structural Engineering Research, Structural Research Division, Korea Institute of Civil Engineering and Building Technology, Republic of Korea.